

Contents

1	Introduction	1
1.1	Overview	1
1.2	Detection Methods	2
1.3	Thesis Focus	9
2	Detecting Exoplanetary Features	10
2.1	Extracting the Signal of features in transit data	10
2.2	Detrending transit data	10
2.3	Model comparison	10
3	Tidal Deformation of Planets	11
3.1	Motivation	11
3.2	Modeling transit of deformed planets	11
3.3	Optimal candidates for detecting tidal deformation	11
3.4	Detectability of planet deformation and measurement of planet Love number	11
3.5	Conclusions	11
4	Exoplanetary Rings	12
4.1	Introduction	12
4.2	Motivation	12
4.3	Techniques	12
4.4	Candidates for Exoring Search	12
4.5	Rings around Low-Density Planets	12
4.6	Conclusions	23
5	Exoplanetary Oblateness	24
5.1	Introduction	24
5.2	Oblate planet transit	25
5.3	Detecting oblateness	29
5.4	Candidates for Oblateness Detection	39
5.5	Conclusions	39
6	Conclusions	40
	Bibliography	41

Chapter 1

Introduction


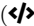

“There are infinite worlds both like and
unlike this world of ours”

(Epicurus, 341–270 BC)

This thesis deals with the search for elusive features that are yet to be detected around exoplanets even though they are expected either from theory or observation of the Solar System planets. In this context, the aim is to contribute to advancing the search for planetary rings, rotation-induced oblateness and tidal deformation in exoplanets, all of which have proved challenging to detect. This first chapter gives a brief overview of the exoplanetary field, the methods by which exoplanets are detected and characterized which will be duly referenced in later chapters relating to induced effects of the aforementioned features. The chapter concludes with the structure of the thesis.¹

1.1 Overview

Humans have long stared at the night sky and wondered about the existence of worlds beyond Earth and even the possibility that some of these could host life. This curiosity is the main motivation of the exoplanet field and continues to drive discoveries in the field till this day. The field really only became prominent and experienced a surge after the discovery of a Jupiter-like exoplanet, 51 Pegasi b, orbiting a Solar-like star (Mayor and Queloz, 1995). The planet orbits much closer to its star than any of the Solar System planets at a distance of only 0.05 AU (Astronomical Units) and a period of 4.2 days (Mercury’s orbit is over 7 times farther from the Sun with a period of 88 days). This discovery was revolutionary, and was awarded the 2019 Nobel prize in Physics, because it challenged the theoretical expectations of planetary systems architecture and paved the way for many more exoplanet detections. Once it was found that giant planets could orbit close to their stars and not only in distant cool regions of the system, the gateway to exoplanet discoveries was immediately flung open. Now exoplanets are literally everywhere, numbering over 4300, with incredibly diverse properties than is seen within the Solar System.

¹For reproducibility of results and plots, links to **Jupyter** notebooks () or **Python** code () are given where necessary throughout the thesis. The Jupyter notebook for the plots in the introduction can be found here 

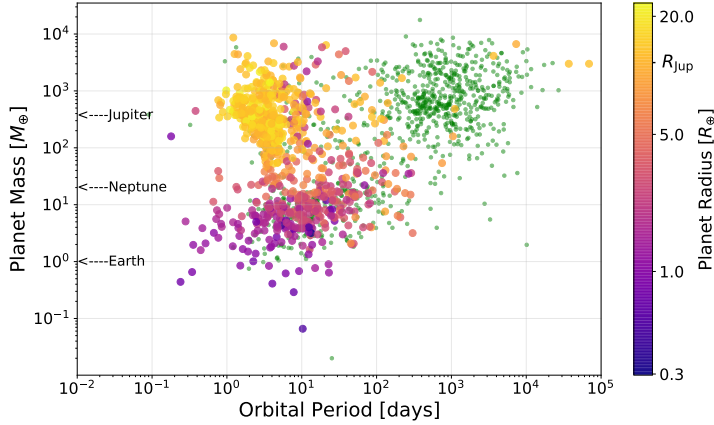


Figure 1.1: Period-Mass-Radius plot of confirmed exoplanets. Green points represent planets without radius measurements. Data from [NASA Exoplanet archive](#)

Figure 1.1 shows the diversity of exoplanets in orbital period, mass, and radius. Their radii and masses range widely from less than that of Earth to a few times greater than Jupiter. Exoplanets can be classified according to their masses - those in the mass range $2\text{--}10 M_{\oplus}$ (Earth masses) as referred to as Super-Earths, those between $10\text{--}100 M_{\oplus}$ as Neptunes and beyond $100 M_{\oplus}$ as Jupiters. The deuterium burning limit of $\sim 13 M_{\text{Jup}}$ (Jupiter masses) sets the maximum mass of a planet before it is considered a brown dwarf or low mass star ([Spiegel et al., 2011](#)). In fig. 1.1, the cluster of high mass and radius planets with periods less than 10 days are referred to as hot-jupiters, similar to the case of 51 Peg b. These planets are highly irradiated by their host stars thereby raising their equilibrium temperatures and partly responsible for the inflation of their radii ([Dawson and Johnson, 2018](#)). A second cluster of planets can also be noticed corresponding to a population of hot or warm Super-Earths and Neptunes with periods less than 100 days while the third visible cluster are Jupiter-sized planets with long orbital periods. Ultimately, the direction is going towards detection of terrestrial planets in the habitable zone of its star, which is a distance from the star where the planetary conditions allow water to exist in liquid form.

It is important to note that the apparent populations of the detected planets are heavily influenced by our current detection methods which are sensitive to different types of planets as will be discussed in the next section.

1.2 Detection Methods

There are several methods used to detect exoplanets. As shown in fig 1.2, the majority of exoplanets have been detected using the transit and Radial Velocity (RV) methods. This section presents an overview of both methods as they are the main methods used in the scope of this thesis (see e.g. [Perryman 2018](#) for a description of the other methods). Together, both methods provide complementary information that allows for better characterisation of exoplanets.

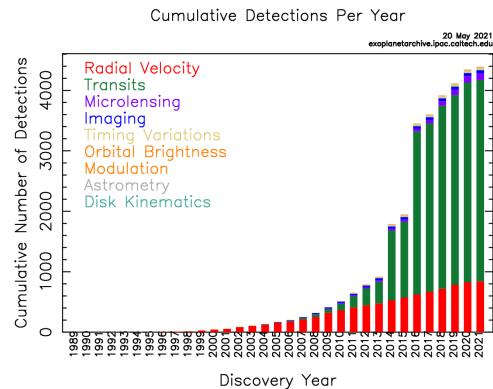


Figure 1.2: Cumulative number of exoplanet detections by year and method. Courtesy: [NASA Exoplanet archive](#)

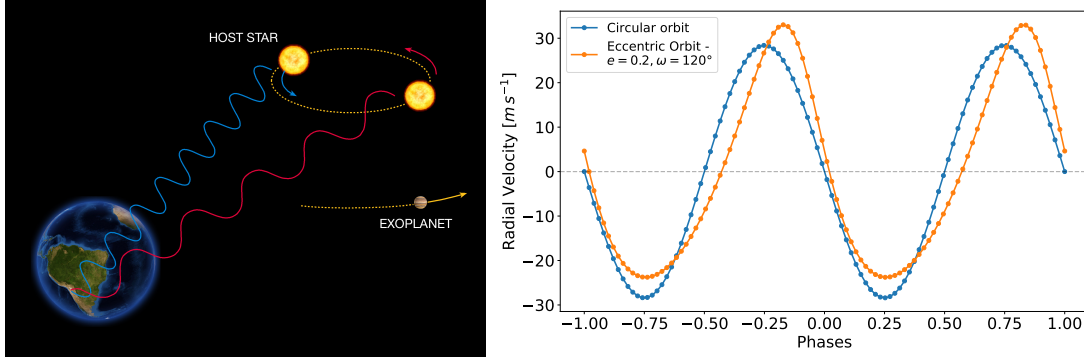


Figure 1.3: Left: Schematic of the radial velocity method (Courtesy: [ESO](#)). Right: RV signal of a Jupiter-mass planet with a Period of 1 yr (Simulated using the *RadVel* package; [Fulton et al. 2018](#)). The impact of eccentricity on the observed RV shape is shown.

1.2.1 Radial Velocity (RV) Method

Radial Velocity method takes credit for the 1995 discovery of 51 Peg b and it remained the major exoplanet discovery method for more than a decade until it was surpassed by the transit method particularly due to the barrage of discoveries enabled by the *Kepler* space telescope ([Borucki et al., 2010](#)).

The presence of a planet around a star causes both the planet and star to orbit the barycenter (center-of-mass) of the system. This holds true for any other stellar companion. As the star is significantly more massive than the planet, the location of the barycenter is closer to the star, usually within the star or close to its surface. The RV method finds planets by searching for Doppler shifts in the spectral lines of the star as it moves towards and away from the observer due to gravitational interaction with the planet. As depicted in the left panel of fig. 1.3, when the star approaches the observer, its spectral lines are shifted from their rest frame wavelength towards shorter wavelengths (blue-shift), whereas when the star recedes, the lines are red-shifted to longer wavelengths. The shift in wavelength, $\Delta\lambda$, compared to the rest frame value, λ , is given, in the non-relativistic limit, by

$$\frac{\Delta\lambda}{\lambda} = \frac{\nu_r}{c}, \quad (1.1)$$

where c is the speed of light and ν_r is the line-of-sight (radial) velocity of the star relative to the observer which depends on the orbital inclination of the planet, i_p . Thus, $\Delta\lambda$ is negative when the lines are blue-shifted and positive when red-shifted. The radial velocity signal is given by

$$\nu_r = K [\cos(\omega + f) + e \cos \omega] + \gamma, \quad (1.2)$$

referred to as a Keplerian function where γ is the proper motion of the barycenter, e is the eccentricity, ω is the argument of periastron, and f is the true anomaly. The semi-amplitude of the RV signal, K , for a planet with period, P , around a star of mass, M_* , is given by

$$K = \frac{28.4 \text{ m s}^{-1}}{\sqrt{1 - e^2}} \frac{M_p \sin i_p}{M_{\text{Jup}}} \left(\frac{M_*}{M_{\odot}} \right)^{-2/3} \left(\frac{P}{1 \text{ yr}} \right)^{-1/3}. \quad (1.3)$$

This equation implies that the RV method favors the detection of more massive and shorter period

planets since they induce larger RV variations. A Jupiter-, Neptune-, and Earth-mass planet with an orbital period of 1 yr around a Solar-mass star will produce RV variations with semi-amplitude of 28.4, 1.53 and 0.9 m s^{-1} respectively. The right pane of fig 1.3 shows the simulated RV signal of a Jupiter-mass planet with $P = 1 \text{ yr}$ and compares the RV signal shape for a circular orbit and an eccentric one with $e = 0.2$ and $\omega = 120^\circ$. Equation 1.3 also reveals that, when M_* is known (through spectroscopic or asteroseismic observations), the RV method can only determine the minimum mass of a planet, $M_p \sin i_p$, due to the unknown component of the stellar velocity perpendicular to the line-of-sight. For this reason, the observed RV variation can either be due to a low-mass planet with an orbital inclination close to 90° or a higher-mass planet with lesser inclination. Measuring i_p from transit observation is thus necessary to obtain the true planetary mass M_p . Furthermore, the RV signal is amplified for planets around less massive stars which has motivated several searches for planets around M-dwarfs (e.g. [Reiners et al. 2018](#)) which are also the most populous stars in our galaxy.

When there is more than one planet in the system, the total RV signal can be approximated by the sum of contributions (Keplerians) from each planet if mutual gravitational interaction between the planets is negligible.

1.2.2 Transit Method

The transit method is responsible for the discovery of a large number of exoplanets (3335, as at June 2021). A transit occurs when a planet passes in front of its host star from the perspective of the observer. When this occurs, the planet blocks a fraction of the stellar light causing a temporary dimming of the star's brightness. Detecting a planet by the transit method thus involves monitoring the brightness of the star in search for a periodic dip in its brightness associated with the passage of a planet. A transit light-curve is produced from the measurement of the stellar flux as a function of time. The depth of the transit, δ , is related to the area of stellar disc covered by the planet and therefore provides a measure of the planet-to-star radius ratio. For a uniform intensity star, the transit depth is given by

$$\delta \simeq \left(\frac{R_p}{R_*} \right)^2, \quad (1.4)$$

where R_p and R_* are the radii of the planet and star respectively. This shows that it is easier to detect larger planets with the transit method since they cause deeper transits. A Jupiter-sized planet transiting a Solar-like star would cause a transit depth of $\sim 1\%$. The transit will be even deeper if the star were smaller, making M-dwarfs once again good targets for detecting exoplanets, particularly Earth-sized ones. Combining radius measurements from transit and mass measurement from RV finally allows astronomers to estimate the bulk densities of exoplanets and compare them to those of the Solar-System planets determining if a planet is rocky or contains significant amounts of volatiles.

The first planet to be detected with the transit method was HD 209458 b ([Charbonneau et al., 2000](#); [Henry et al., 2000](#)). With a derived radius of $1.27 R_{\text{Jup}}$, it confirmed that the Jupiter-mass objects detected in RV were indeed Jupiter-sized giant planets with similar densities. Figure 1.4 shows the transit light-curve of HD 209458 b ([Charbonneau et al., 2000](#)). The number of transiting planet grew rapidly after this detection with follow-ups of RV detected planets and ground-based transit surveys such as HATNet ([Bakos et al., 2002](#)), OGLE ([Udalski et al., 2003](#)), WASP ([Pollacco et al., 2006](#)) and TrES ([Alonso](#)

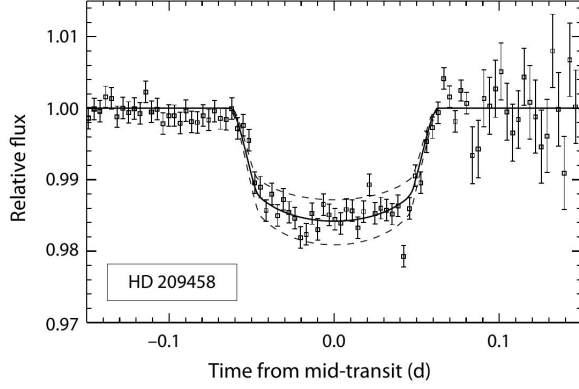


Figure 1.4: Light-curve of the first detected transiting exoplanet HD 209458 b (Charbonneau et al., 2000).

et al., 2004) which had sufficient precision to detect these giant planets. The first space-based transit observation was that of HD 209458 b using the Hubble Space Telescope (Brown et al., 2001) revealing the power of space-based photometry for providing highly precise photometry capable of particularly searching for features such as rings and moons.

Besides the transit depth from which the R_p/R_* is derived, there are other observables from transit observations that allow to derive more planetary and orbital parameters. These observables are: the total transit duration T_t , duration of full transit T_f , and for multiple transits, the period. From these, Seager and Mallen-Ornelas (2003) showed that, for circular orbit, it is possible to derive the scaled semi-major axis of the planet orbit as

$$\frac{a}{R_*} = \left\{ \frac{(1 + R_p/R_*)^2 - b^2[1 - \sin^2(T_t\pi/P)]}{\sin^2(T_t\pi/P)} \right\}^{1/2}, \quad (1.5)$$

where b is the impact parameter of the transit defined as the sky-projected distance between the centers of the star and planet at mid-transit. It is given as

$$b = \frac{a}{R_*} \cos i_p, \quad (1.6)$$

and allows us estimate the inclination i_p of the planetary orbit, which can be combined with RV observation to determine a planet's true mass.

Furthermore, with Kepler's third law given by

$$P^2 = \frac{4\pi^2 a^3}{G(M_* + M_p)}, \quad (1.7)$$

it is possible to obtain a transit-derived stellar density assuming that $M_p \ll M_*$ which is usually satisfied. This is done by substituting $\rho_* = 3M_*/4\pi R_*^3$ in eqn 1.7 giving:

$$\rho_* = \frac{3\pi}{GP^2} \left(\frac{a}{R_*} \right)^3. \quad (1.8)$$

This is an independent method of estimating stellar density, separate from asteroseismology, using only the light-curve parameters. Conversely, in fitting transit light-curve, the known stellar density can be used to place prior constraints the value of a/R_* (which indirectly determines the transit duration

T_t). See [Kipping \(2010\)](#) for modifications to equations 1.5–1.8 for an eccentric orbit.

Clearly, transit observations provide us with a treasure trove of information, but there's a catch: the orbit of a planet needs to be properly aligned in order for a transit to occur. The probability that a transit occurs is given (e.g. in [Perryman 2018](#)) by

$$P_{\text{tr}} = \left(\frac{R_* \pm R_p}{a} \right) \left(\frac{1}{1 - e^2} \right). \quad (1.9)$$

The '+' or '-' sign allows for grazing transits or excludes them. The probability implies that planet with closer to their stars are more likely to transit. The large sizes and proximity of hot-Jupiters makes them ideal for transit detections which explains the cluster of these planets in fig. 1.1.

Limb darkening: In equation 1.4, the transit depth assumes that the stellar intensity is uniform. In reality, the stellar disc is brighter at the center and darkens progressively towards the limb. This means that the transit will be deeper at mid-transit due to limb darkening since the planet obscures more stellar intensity at the center than any other region. Limb darkening thus causes a rounder transit bottom. Limb darkening occurs due to the stratification in stellar density and temperature with altitude. When observing a transit, the line-of-sight towards the limb is oriented at an angle θ from the normal to the stellar surface causing an optical depth of unity to be attained at a higher altitude where the stellar temperature and intensity are lower.

The limb darkening is usually represented as a function of $\mu = \cos \theta$ ($\mu = 1$ at the center of the stellar disc and zero at the limb). Several parametric limb darkening laws have been proposed which attempt to approximate the intensity profile of stellar atmospheric models. Some examples of popular limb darkening laws are:

The quadratic law ([Kopal, 1950](#)):

$$I(\mu)/I(1) = 1 - u_1(1 - \mu) - u_2(1 - \mu)^2 \quad (1.10)$$

The square-root law ([Diaz-Cordovez and Gimenez, 1992](#)):

$$I(\mu)/I(1) = 1 - u_1(1 - \mu) - u_2(1 - \sqrt{\mu}) \quad (1.11)$$

The power-2 law ([Hestroffer, 1997](#); [Maxted, 2018](#)):

$$I(\mu)/I(1) = 1 - u_1(1 - \mu^{u_2}) \quad (1.12)$$

Four parameter law ([Claret, 2000](#)):

$$I(\mu)/I(1) = 1 - \sum_{i=1}^4 u_i(1 - \mu^{i/2}) \quad (1.13)$$

The three-parameter law: (Sing et al., 2009):

$$I(\mu)/I(1) = 1 - \sum_{i=2}^4 u_i (1 - \mu^{i/2}) \quad (1.14)$$

where $I(1)$ is the intensity at the center of the disc and u_i are the limb darkening coefficients (LDCs) of for each law. As limb darkening modifies the shape of a light-curve, it can affect the inferred parameters like the radius ratio and other higher-order effects such as those sought-after in this thesis (Csizmadia et al., 2013; Short et al., 2019). Therefore, accurate treatment of limb darkening is crucial especially for very precise transit measurements (Kipping, 2013; Espinoza and Jordán, 2015).

Transit Timing and Transit Duration Variations:

Transiting planets in multiplanetary systems may have non-keplerian orbits due to gravitational interaction between the planets. Such interactions meddle with the usual clock-work precision of periodic transits and can lead to transit timing variations (TTV) and transit duration variations (TDV).

If the transit of a planet is detected, deviations from a linear ephemeris can reveal the presence of an additional planet in the system, even if non-transiting, and also allow determination of its mass, period and eccentricity (Agol et al., 2005; Holman and Murray, 2005; Nesvorný, 2019). TTVs are stronger for planets near mean-motion resonances in which the ratio of periods of two planets is close to the ratio of small integers. The first significant TTV detection was in the Kepler-9 system which showed large-amplitude TTVs due to two Saturn-sized planets (Holman et al., 2010). After that, TTVs have been observed in more than 100 systems (Holczer et al., 2016). The first case of discovery and completely characterization of a non-transiting planet was for Kepler- 46 (Nesvorný et al., 2012).

One source of TDV is variation in orbital eccentricity of a planet due to resonant interaction. Variation in eccentricity causes variations in the the speed and length of transit thereby modifying the transit duration between consecutive transits. This has been observed in KOI-142 (Nesvorný et al., 2013) where the TTVs and TDVs were used to detect the non-transiting companion KOI-142c.

Additionally, the presence of a moon around an exoplanet (exomoon) could cause observable TTVs and TDVs since a moon gravitationally perturbs the planet along its orbit. TTVs and TDVS have even be proposed as methods to detect them (Kipping, 2009a,b).

Rossiter-McLaughlin signal:

In addition to the photometric signal of a transiting planet, a spectroscopic transit signal can be obtained from the measurement of the star's radial velocity shift during planetary transit. When a star is rotating, half of the stellar disc approaches the observer while the other half recedes from the observer. Due to Doppler effect, light from the approaching half will appear blue-shifted while light from the receding half will appear red-shifted (see Fig. 1.5). Without a transit, the stellar rotation causes the spectral lines to be broadened but this does not lead to an overall doppler shift since the effect from both halves of stellar disc will average out when integrated. However, when a planet transits the star, it blocks part of the blueshifted half causing the disc-integrated stellar light to be slightly redshifted. The same occurs

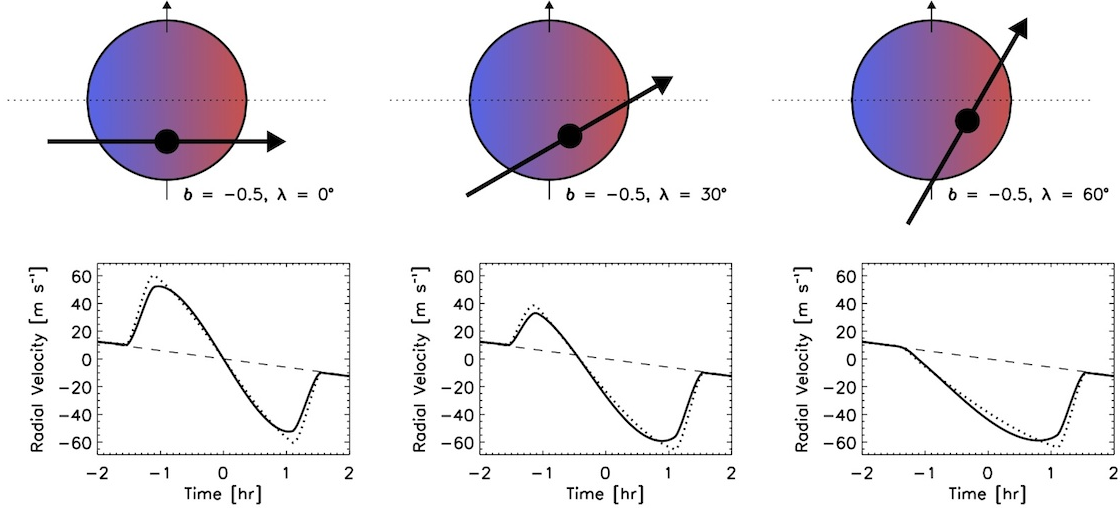


Figure 1.5: Top: Transits of a planet across a rotating star with three different paths (defined by angle λ between projected planet orbit and stellar spin axis). Bottom: The different RM signals produced by the three planet orbit paths. The long dashed line shows the star's RV without a transiting planet. Solid and dotted curves show the RM signals with and without limb darkening. From [Gaudi and Winn \(2007\)](#).

when it blocks part of the redshifted half leading to a slightly blueshifted integrated stellar light.

As the planet transits across the stellar disc, it covers different regions with varying radial velocity components thereby causing a RV anomaly referred to as the Rossiter-McLaughlin (RM) effect ([Rossiter, 1924](#); [McLaughlin, 1924](#)). Figure 1.5 illustrates the RM signals for a planet with same parameters but following different paths across the star. The three paths would produce the same transit light-curve but different RM signals, so the RM signal can give us extra information about a transiting planet. Since the RM effect is sensitive to the planet's transit path, it offers information about the projected angle between the planet orbit and the stellar equator called the spin-orbit angle, λ . It also allows measurement of the projected stellar rotational velocity, $\nu \sin i_*$. As seen in the bottom plots of fig. 1.5, the RM signal of the well-aligned planet ($\lambda=0^\circ$) is anti-symmetric about the midtransit time whereas that of the misaligned planets will either be asymmetric ($\lambda=30^\circ$) or produce the anomaly from only one of the hemispheres ($\lambda=60^\circ$).

The amplitude of RM effect, A_{RM} , is given (e.g. by [Gaudi and Winn 2007](#)) as

$$A_{RM} \simeq \nu \sin i_* \left(\frac{R_p}{R_*} \right)^2 \sqrt{(1 - b^2)} \quad (1.15)$$

The RM effect is most significant for large planets transiting fast rotating stars. [Queloz et al. \(2000\)](#) was the first to report observation of the RM effect for an exoplanet, HD 209458 b, measuring a spin-orbit angle of 3.9° . Spin-orbit angle measurements using RM observations are now regularly obtained and it has shown that exoplanets have a large diversity in λ , from aligned to highly misaligned and even retrograde systems ([Hébrard et al., 2008](#); [Anderson et al., 2015](#); [Esposito et al., 2014](#)). The distribution of spin-orbit angle can help inform migration theories and histories of exoplanets ([Winn et al., 2010](#)).

1.3 Thesis Focus

In deriving some of the exoplanet parameters and properties above, specifically for transiting planets, an implicit assumption has been made that the exoplanet is spherical and has no extended features. However, a departure from sphericity due to tidal deformation, oblateness and rings could alter the relationship between these parameters and impact the shape of the observed transit light-curve and RM signal. As instrumental precisions increase, the subtle effects of these features in transit data begin to get more prominent thereby better allowing their detection and proper characterisation.

This manuscript is composed of three distinct parts, each dealing with a different investigation of how exoplanetary transits can be used to detect and characterize tidal deformation, rings and oblateness. Therefore, the thesis should be more appropriately titled ”*Looking for rings and shape deformation in transiting exoplanets*”.

In Chapter 2, I lay the ground work for identifying the signature of features in transit data, detrending methods that preserve these signatures and Bayesian approach to comparing models with and without the sought-after features. In Chapter 3, I adapt a transit tool to model the light-curve of tidally deformed planets and use this tool to investigate the detectability of tidal deformation in short-period planets and identify favorable targets. I also show how detecting tidal deformation allows to gain insight into the interior structure of planets and other prospects. Chapter 4 is an investigation into the detection of exoplanetary rings, updates to the ringed planet transit tool SOAP3.0, effects of rings to transit signals and the derived parameters, identification of suitable candidates and an analysis of a specific case. Chapter 5 investigates the signature of rotation-induced oblateness showing that the induced signal in spectroscopy can complement that from photometry and also presents analysis of some candidates. Finally in Chapter 6, I present the conclusions of my work and future outlook for the detection of these features.

Bibliography

- Agol, E., Steffen, J., Sari, R., and Clarkson, W.: 2005, *Monthly Notices of the Royal Astronomical Society* **359**(2), 567
- Alonso, R., Brown, T. M., Torres, G., Latham, D. W., Sozzetti, A., Mandushev, G., Belmonte, J. A., Charbonneau, D., Deeg, H. J., Dunham, E. W., O'Donovan, F. T., and Stefanik, R. P.: 2004, *The Astrophysical Journal* **613**(2), L153
- Anderson, D. R., Triaud, A. H. M. J., Turner, O. D., Brown, D. J. A., Clark, B. J. M., Smalley, B., Cameron, A. C., Doyle, A. P., Gillon, M., Hellier, C., Lovis, C., Maxted, P. F. L., Pollacco, D., Queloz, D., and Smith, A. M. S.: 2015, *The Astrophysical Journal* **800**(1), L9
- Bakos, G. , Lázár, J., Papp, I., Sári, P., and Green, E. M.: 2002, *Publications of the Astronomical Society of the Pacific* **114**(799), 974
- Borucki, W. J., Koch, D., Basri, G., Batalha, N., Brown, T., Caldwell, D., Caldwell, J., Christensen-Dalsgaard, J., Cochran, W. D., Devore, E., Dunham, E. W., Dupree, A. K., Gautier, T. N., Geary, J. C., Gilliland, R., Gould, A., Howell, S. B., Jenkins, J. M., Kondo, Y., Latham, D. W., Marcy, G. W., Meibom, S., Kjeldsen, H., Lissauer, J. J., Monet, D. G., Morrison, D., Sasselov, D., Tarter, J., Boss, A., Brownlee, D., Owen, T., Buzasi, D., Charbonneau, D., Doyle, L., Fortney, J., Ford, E. B., Holman, M. J., Seager, S., Steffen, J. H., Welsh, W. F., Rowe, J., Anderson, H., Buchhave, L., Ciardi, D., Walkowicz, L., Sherry, W., Horch, E., Isaacson, H., Everett, M. E., Fischer, D., Torres, G., Johnson, J. A., Endl, M., MacQueen, P., Bryson, S. T., Dotson, J., Haas, M., Kolodziejczak, J., Van Cleve, J., Chandrasekaran, H., Twicken, J. D., Quintana, E. V., Clarke, B. D., Allen, C., Li, J., Wu, H., Tenenbaum, P., Verner, E., Bruhweiler, F., Barnes, J., and Prsa, A.: 2010, *Science* **327**(5968), 977
- Brown, T. M., Charbonneau, D., Gilliland, R. L., Noyes, R. W., and Burrows, A.: 2001, *The Astrophysical Journal* **552**(2), 699
- Charbonneau, D., Brown, T. M., Latham, D. W., and Mayor, M.: 2000, *The Astrophysical Journal* **529**(1), L45
- Claret, A.: 2000, *Astronomy and Astrophysics* **363**(3), 1081
- Csizmadia, S., Pasternacki, T., Dreyer, C., Cabrera, J., Erikson, A., and Rauer, H.: 2013, *Astronomy & Astrophysics* **549**, A9
- Dawson, R. I. and Johnson, J. A.: 2018, *Origins of Hot Jupiters*

- Diaz-Cordovez, J. and Gimenez, A.: 1992, *Astronomy and astrophysics (Berlin. Print)* **259(1)**, 227
- Espinoza, N. and Jordán, A.: 2015, *Monthly Notices of the Royal Astronomical Society* **450(2)**, 1879
- Esposito, M., Covino, E., Mancini, L., Harutyunyan, A., Southworth, J., Biazzo, K., Gandolfi, D., Lanza, A. F., Barbieri, M., Bonomo, A. S., Borsa, F., Claudi, R., Cosentino, R., Desidera, S., Gratton, R., Pagano, I., Sozzetti, A., Boccato, C., Maggio, A., Micela, G., Molinari, E., Nascimbeni, V., Piotto, G., Poretti, E., and Smareglia, R.: 2014, *Astronomy and Astrophysics* **564**, 13
- Fulton, B. J., Petigura, E. A., Blunt, S., and Sinukoff, E.: 2018, *Publications of the Astronomical Society of the Pacific* **130(986)**, 044504
- Gaudi, B. S. and Winn, J. N.: 2007, *The Astrophysical Journal* **655(1)**, 550
- Hébrard, G., Bouchy, F., Pont, F., Loeillet, B., Rabus, M., Bonfils, X., Moutou, C., Boisse, I., Delfosse, X., Desort, M., Eggenberger, A., Ehrenreich, D., Forveille, T., Lagrange, A. M., Lovis, C., Mayor, M., Pepe, F., Perrier, C., Queloz, D., C. Santos, N., Ségransan, D., Udry, S., and Vidal-Madjar, A.: 2008, *Astronomy and Astrophysics* **488(2)**, 763
- Henry, G. W., Marcy, G. W., Butler, R. P., and Vogt, S. S.: 2000, *The Astrophysical Journal* **529(1)**, L41
- Hestroffer, D.: 1997, *Astronomy and Astrophysics* **327(1)**, 199
- Holczer, T., Mazeh, T., Nachmani, G., Jontof-Hutter, D., Ford, E. B., Fabrycky, D., Ragozzine, D., Kane, M., and Steffen, J. H.: 2016, *The Astrophysical Journal Supplement Series* **225(1)**, 9
- Holman, M. J., Fabrycky, D. C., Ragozzine, D., Ford, E. B., Steffen, J. H., Welsh, W. F., Lissauer, J. J., Latham, D. W., Marcy, G. W., Walkowicz, L. M., Batalha, N. M., Jenkins, J. M., Rowe, J. F., Cochran, W. D., Fressin, F., Torres, G., Buchhave, L. A., Sasselov, D. D., Borucki, W. J., Koch, D. G., Basri, G., Brown, T. M., Caldwell, D. A., Charbonneau, D., Dunham, E. W., Gautier, T. N., Geary, J. C., Gilliland, R. L., Haas, M. R., Howell, S. B., Ciardi, D. R., Endl, M., Fischer, D., Fürész, G., Hartman, J. D., Isaacson, H., Johnson, J. A., MacQueen, P. J., Moorhead, A. V., Morehead, R. C., and Orosz, J. A.: 2010, *Science* **330**, 51
- Holman, M. J. and Murray, N. W.: 2005, *Science* **307(5713)**, 1288
- Kipping, D. M.: 2009a, *Monthly Notices of the Royal Astronomical Society* **392(1)**, 181
- Kipping, D. M.: 2009b, *Monthly Notices of the Royal Astronomical Society* **396(3)**, 1797
- Kipping, D. M.: 2010, *Monthly Notices of the Royal Astronomical Society* **407(1)**, 301
- Kipping, D. M.: 2013, *Monthly Notices of the Royal Astronomical Society* **435(3)**, 2152
- Kopal, Z.: 1950, *Harvard College Observatory Circular* **454**, 1
- Maxted, P. F.: 2018, *Astronomy and Astrophysics* **616**, 39
- Mayor, M. and Queloz, D.: 1995, *\nat* **378**, 355
- McLaughlin, D. B.: 1924, *\apj* 60

Nesvorný, D.: 2019, *New Astronomy Reviews* **84**, 101507

Nesvorný, D., Kipping, D., Terrell, D., Hartman, J., Bakos, G. , and Buchhave, L. A.: 2013, *Astrophysical Journal* **777**(1), 3

Nesvorný, D., Kipping, D. M., Buchhave, L. A., Bakos, G. , Hartman, J., and Schmitt, A. R.: 2012, *Science* **336**, 1133

Perryman, M.: 2018, *The Exoplanet Handbook*, Cambridge University Press

Pollacco, D., Skillen, I., Cameron, A., Christian, D., Irwin, J., Lister, T., Street, R., West, R., Clarkson, W., Evans, N., Fitzsimmons, A., Haswell, C., Hellier, C., Hodgkin, S., Horne, K., Jones, B., Kane, S., Keenan, F., Norton, A., Osborne, J., Ryans, R., and Wheatley, P.: 2006, in *Astrophysics and Space Science*, Vol. 304, pp 253–255, Springer

Queloz, D., Eggenberger, A., Mayor, M., Perrier, C., Beuzit, J. L., Naef, D., Sivan, J. P., and Udry, S.: 2000, *Astronomy and Astrophysics* 359(2)

Reiners, A., Zechmeister, M., Caballero, J. A., Ribas, I., Morales, J. C., Jeffers, S. V., Schöfer, P., Tal-Or, L., Quirrenbach, A., Amado, P. J., Kaminski, A., Seifert, W., Abril, M., Aceituno, J., Alonso-Floriano, F. J., Ammler-Von Eiff, M., Antona, R., Anglada-Escudé, G., Anwand-Heerwart, H., Arroyo-Torres, B., Azzaro, M., Baroch, D., Barrado, D., Bauer, F. F., Becerril, S., Béjar, V. J., Benítez, D., Berdinas, Z. M., Bergond, G., Blümcke, M., Brinkmüller, M., Del Burgo, C., Cano, J., Cárdenas Vázquez, M. C., Casal, E., Cifuentes, C., Claret, A., Colomé, J., Cortés-Contreras, M., Czesla, S., Díez-Alonso, E., Dreizler, S., Feiz, C., Fernández, M., Ferro, I. M., Fuhrmeister, B., Galadí-Enríquez, D., García-Piquer, A., García Vargas, M. L., Gesa, L., Galera, V. G., González Hernández, J. I., González-Peinado, R., Grözing, U., Grohner, S., Guàrdia, J., Guenther, E. W., Guizarro, A., Guindos, E. D., Gutiérrez-Soto, J., Hagen, H. J., Hatzes, A. P., Hauschildt, P. H., Hedrosa, R. P., Helmling, J., Henning, T., Hermelo, I., Hernández Arabí, R., Hernández Castaño, L., Hernández Hernando, F., Herrero, E., Huber, A., Huke, P., Johnson, E. N., Juan, E. D., Kim, M., Klein, R., Klüter, J., Klutsch, A., Kürster, M., Lafarga, M., Lamert, A., Lampón, M., Lara, L. M., Laun, W., Lemke, U., Lenzen, R., Launhardt, R., López Del Fresno, M., López-González, J., López-Puertas, M., López Salas, J. F., López-Santiago, J., Luque, R., Magán Madinabeitia, H., Mall, U., Mancini, L., Mandel, H., Marfil, E., Marín Molina, J. A., Maroto Fernández, D., Martín, E. L., Martín-Ruiz, S., Marvin, C. J., Mathar, R. J., Mirabet, E., Montes, D., Moreno-Raya, M. E., Moya, A., Mundt, R., Nagel, E., Naranjo, V., Nortmann, L., Nowak, G., Ofir, A., Oreiro, R., Pallé, E., Panduro, J., Pascual, J., Passegger, V. M., Pavlov, A., Pedraz, S., Pérez-Calpena, A., Medialdea, D. P., Perger, M., Perryman, M. A., Pluto, M., Rabaza, O., Ramón, A., Rebolo, R., Redondo, P., Reffert, S., Reinhart, S., Rhode, P., Rix, H. W., Rodler, F., Rodríguez, E., Rodríguez-López, C., Rodríguez Trinidad, A., Rohloff, R. R., Rosich, A., Sadegi, S., Sánchez-Blanco, E., Sánchez Carrasco, M. A., Sánchez-López, A., Sanz-Forcada, J., Sarkis, P., Sarmiento, L. F., Schäfer, S., Schmitt, J. H., Schiller, J., Schweitzer, A., Solano, E., Stahl, O., Strachan, J. B., Stürmer, J., Suárez, J. C., Tabernero, H. M., Tala, M., Trifonov, T., Tulloch, S. M., Ulbrich, R. G., Veredas, G., Vico Linares, J. I., Vilardell, F., Wagner, K., Winkler, J., Wolthoff, V., Xu, W., Yan, F., and Zapatero Osorio, M. R.: 2018, *Astronomy and Astrophysics* 612

Rossiter, R. A.: 1924, \apj 60

- Seager, S. and Mallen-Ornelas, G.: 2003, *The Astrophysical Journal* **585(2)**, 1038
- Short, D. R., Welsh, W. F., Orosz, J. A., Windmiller, G., and Maxted, P. F. L.: 2019, *Research Notes of the AAS* **3(8)**, 117
- Sing, D. K., Désert, J. M., Lecavelier Des Etangs, A., Ballester, G. E., Vidal-Madjar, A., Parmentier, V., Hebrard, G., and Henry, G. W.: 2009, *Astronomy and Astrophysics* **505(2)**, 891
- Spiegel, D. S., Burrows, A., and Milsom, J. A.: 2011, *Astrophysical Journal* **727(1)**, 57
- Udalski, A., Pietrzyński, G., Szymański, M., Kubiak, M., Zebruń, K., Soszyński, I., Szewczyk, O., and Wyrzykowski: 2003, *Acta Astronomica* **53(2)**, 133
- Winn, J. N., Fabrycky, D., Albrecht, S., and Johnson, J. A.: 2010, *Astrophysical Journal Letters* **718(2 PART 2)**, 145